DOI:10.1158/0008-5472.CAN-03-3443

Cancer Research

GW112, A Novel Antiapoptotic Protein That Promotes Tumor Growth

Xiuwu Zhang, Qian Huang, Zhonghui Yang, et al.

Cancer Res 2004;64:2474-2481. Published online April 1, 2004.

DOI:10.1158/0008-5472.CAN-03-3443

[CANCER RESEARCH 64, 2474–2481, April 1, 2004]

GW112, A Novel Antiapoptotic Protein That Promotes Tumor Growth

Xiuwu Zhang,[1] Qian Huang,[1,2] Zhonghui Yang,[1] Yongping Li,[1] and Chuan-Yuan Li[1]

[1]Department of Radiation Oncology, Duke University Medical Center, Durham, North Carolina, and [2]No.1 People's Hospital, Shanghai Jiao Tong University, Shanghai, People's Republic of China

ABSTRACT

***GW112* is a novel gene that has little homology to other known genes. It is overexpressed in a number of human tumor types, especially in those of the digestive system. We show here that *GW112* is associated with GRIM-19, a protein known to be involved in regulating cellular apoptosis. Functionally, *GW112* could significantly attenuate the ability of GRIM19 to mediate retinoic acid-IFN-β-mediated cellular apoptosis and apoptosis-related gene expression. In addition, GW112 demonstrated strong antiapoptotic effects in tumor cells treated with other stress exposures such as hydrogen peroxide. Finally, forced overexpression of *GW112* in murine prostate tumor cells led to more rapid tumor formation in a syngeneic host. Taken together, our data suggest that GW112 is an important regulator of cell death that plays important roles in tumor cell survival and tumor growth.**

INTRODUCTION

Apoptosis, or programmed cell death, is a fundamental process in the development and homeostatic maintenance of biological systems (1, 2). It is a tightly regulated process that is normally initiated to eliminate unwanted cells in multicellular organisms (3). Aberrations in the regulation of this process are involved in various pathological conditions such as cancer (4–8), neurodegenerative diseases (9, 10), autoimmune disorders (11–13), and viral infections (14, 15). Apoptosis played critical roles in carcinogenesis because it is a major hurdle that a normal mammalian cell would have to pass before it becomes carcinogenic (16). Genetic defects in the control of apoptosis allow for the expansion of neoplastic cells. It also enables them to escape immunosurveillance and treatment (chemo- or radiation therapy). Therefore, apoptosis control in cancer cells is of critical biological and clinical importance (17–20).

Tumor cells encounter a wide variety of adverse growth conditions such as hypoxia, low pH, and glucose deprivation (21–23). A normal cell experiencing these stressful conditions will invoke responses such as growth arrest and activation of apoptosis. However, tumor cells can grow despite being under stress. This ability is acquired through genetic/epigenetic alterations in various genes that control several mechanisms, which include apoptosis as well as cell cycle progression. Understanding these alterations may allow us to gain insights into the process of tumor growth that may in turn lead to new targets for therapeutics development.

In our efforts to identify novel differentially expressed genes in cancer cells through the use of National Cancer Institute Cancer Genome Anatomy Project system, we came across the *GW112* (Unigene ID#Hs.273321) gene by virtue of its high expression in human colon tumors. *GW112* was initially cloned from human myeloblasts. However, little is known about its function or structure. It bears little homology to other known genes. There is thus far only a single published report that identified it to be a dominant mRNA species in inflamed colonic epithelium (24). Its expression was confined to the crypt epithelium. Preferential expression of *GW112* in the crypt epithelium of inflamed colonic mucosa in ulcerative colitis suggests an important physiological role of GW112, although its exact function remains unknown.

We conducted a series of experiments to decipher the function of GW112. We show that GW112 is expressed in multiple human normal and malignant tissues with the highest expression in organs/tumors of the digestive system. We also identified, through the yeast two-hybrid system, that GW112 protein interacts with a known protein GRIM-19, which has been implicated in IFN/retinoic acid-induced apoptosis (25–29). We report that overexpression of the *GW112* gene can attenuate hydrogen peroxide and IFN-β/retinoic acid-induced cellular apoptosis and apoptotic gene expression. The overexpression of GW112 also facilitated clonogenic tumor cellular survival and rapid tumor growth. Therefore, our results suggest that GW112 is an important regulator of cellular apoptosis that may be involved in tissue homeostasis and tumor development.

MATERIALS AND METHODS

Cell Culture. We have used the following cells in our studies, HEK 293, an immortalized human embryonic kidney cell line; SVEC4–10, a mouse lymphoid vein endothelial cell transformed by SV40; HeLa, a human adenocarcinoma cell line; and TRAMP-C1 cell line, a mouse prostate tumor cell line. All of the cell lines, with the exception of the last one, were obtained from American Type Culture Collection. The TRAMP-C1 cell line was obtained from Dr. Norman Greenberg of Baylor College of Medicine. The cells were cultured in DMEM (Invitrogen Inc., Carlsbad, CA) with 10% fetal bovine serum, 100 unit/ml penicillin, and 100 μg/ml streptomycin at 37°C, 5% CO_2.

Multiple Tissue Northern Blot Analysis. For Northern blot analysis, we used commercially available eight-lane multiple tumor tissue Northern blots (MTN blots) from the Clontech Corporation (Palo Alto, CA). It contains 10 μg of total RNA samples per lane. The Northern blot analyses of GW112 expression was performed according to the manufacturer's instruction by use of ^{32}P-labeled cDNA probe.

Yeast Two-Hybrid Library Screening. For yeast two-hybrid analysis, we used the Matchmaker Two-Hybrid System 3 and pretransformed Matchmaker kidney library (no library from tissues of the digestive system, which are more preferable, was available at the time of the experiment), both from the Clontech Corporation. The matchmaker kidney library was constructed by use of mRNA extracted from normal, whole kidney. It was built into the pACT2 plasmid and was pretransformed into yeast strain Y187, which provides for expression of library proteins fused to the 3′ terminus of GAL4 transcriptional activation domain (AD). The reverse transcription-PCR derived human GW112 cDNA (GenBank accession no. NM-006418) was cloned into the pGBKT7 vector by fusing the whole coding sequence to the 3′ terminus of the GAL4 DNA-binding domain. pGBKT7-GW112 was then transformed into the yeast strain AH109. The AH109 and Y187 yeast strains were of opposite mating types incorporating four reporter constructs, in which various transcriptional reporter genes (*HIS3*, *ADE2*, *MEL1*, and *lacZ*) were controlled by three heterologous GAL4-responsive upstream activating sequences with their corresponding promoter elements. The AH109 cells that contained the GW112-binding domain fusion protein were then mated with the Y187 cells with the cDNA-AD fusion library. The mating was performed essentially as described in the product manual provided by Clontech. The activation of transcriptional reporters was then assessed by plating the mating mixture on medium- and

Received 11/4/03; revised 1/13/04; accepted 1/22/04.

Grant support: Grant CA81512 from the National Cancer Institute and a grant from the Komen Foundation for Breast Cancer Research (C-Y. Li).

The costs of publication of this article were defrayed in part by the payment of page charges. This article must therefore be hereby marked *advertisement* in accordance with 18 U.S.C. Section 1734 solely to indicate this fact.

Note: X. Zhang is a W. Osborn Lee Fellow at the Duke University Comprehensive Cancer Center.

Requests for reprints: Chuan-Yuan Li, Department of Radiation Oncology, Duke University Medical Center, Durham, NC 27710. Phone: (919) 684-8718; Fax: (919) 684-8718; E-mail: cyli@radonc.duke.edu.

DOI:10.1158/0008-5472.CAN-03-3443

high-stringency synthetic dropout medium. Medium-stringency medium, lacking histidine, required activation of the *HIS3* reporter to permit colony growth. The high-stringency medium, on the other hand, required activation of both HIS3 and ADE2 reporters for growth to occur. All of the plates also contained 20 μg/ml X-α-gal (Clontech Inc.), a chromogenic substrate that makes the yeast colonies blue when they had their MEL1 reporter gene activated. The positive colonies (those that appeared blue) were retested for phenotypes. The plasmids from positive colonies were then isolated after transformation into *Escheria coli*, and the interaction was confirmed in yeast by mating. Plasmids from different positive colonies were sequenced, and the in-frame cDNAs were selected for mammalian two-hybrid assay and *in vivo* coimmunoprecipitation assay.

Mammalian Two-Hybrid Assay. For mammalian two-hybrid analysis, we used the Mammalian Matchmaker Two-Hybrid assay kit (BD Clontech). The human *GW112* cDNA (NM-006418) was cloned into the pM vector (to derive pBD-GW112) to generate a fusion protein between the GW112 protein and the yeast GAL4 DNA binding domain. The human GRIM-19 cDNA was cloned into the pVP16 vector (to derive pAD-GRIM-19) to generate a fusion protein between GRIM-19 and the transcription AD of VP16 (VP16-AD). If there is potential interaction between GW112 and GRIM-19, the complex formed between the two fusion proteins will result in a full-fledged transcriptional factor that can activate any reporter genes that possess GAL4 binding domains. The reporter adopted in the Clontech kit was a CAT gene (G5CAT) that contains five consensus GAL4 binding site and a minimal promoter of adenovirus *E1b* gene. To detect potential interaction between GW112 and GRIM-19, the three plasmids, pBD-GW112, pAD-GRIM-19, and G5CAT, were cotransfected into 60–70% confluent 293 cells using the LipofectAMINE (Invitrogen Inc., Carlsbad, CA). Forty-eight to 72 h later, the cells were harvested by use of a cell lysis buffer provided in a CAT ELISA kit purchased from Roche Molecular Biology (Mannheim, Germany). The cells lysate was then centrifuged, and the supernatant was used for CAT activities assay according to manufacturer's instruction.

***In Vivo* Coimmunoprecipitation.** For *in vivo* coimmunoprecipitation, the human GRIM-19 cDNA was cloned into pCMV-Tag-2B Epitope Tagging mammalian Expression Vector (Stratagene, La Jolla, CA). A FLAG epitope tag was located at the NH_2 terminal of the protein. The human GW112 cDNA (NM-006418) was engineered (through PCR) to have a hemagglutin (HA) epitope in the 3′ end and was subsequently cloned into pCMV-Tag-2B without fusion to the Flag epitope. The two plasmids were cotransfected into 293 cells at 70–80% confluency. The cells were detached and collected in 500 μl of immunoprecipitation buffer [20 mM sodium phosphate, (pH 7.5), 500 mM NaCI, 0.1% SDS, 1% NP40, 0.5% sodium deoxycholate, and 0.02% sodium azide] 48 h later. After the cells were lysed, the supernatant (400 μl) was incubated with 8 μl anti-HA antibody (1:50 dilution) overnight at 4°C. Afterward, ~100 μl of Ultralink Immobilized protein G (Pierce, Rockford, IL) was added and gently mixed for 2 h at room temperature. The beads were washed six to eight times with 1 ml immunoprecipitation buffer and boiled in 50 μl of the SDS/sample buffer for 5–8 min. After a brief precipitation (spin down), the supernatant (10 μl) was run in a 14% SDS-PAGE gel for Western blot analysis by use of an antiflag antibody (1:1000; Stratagene Inc.).

Plasmid Construction and Adenovirus Production. The AdEasy system of adenovirus packaging, including plasmid pAdtrack-CMV, pAdeasy-1, and the packaging *E. coli* BJ5183 cells, was kindly provided by Dr. Tong-Chuan He (The Johns Hopkins University School of Medicine, Baltimore, MD; Ref. 30). The human *GW112* gene was amplified by reverse transcription-PCR from total RNA of human colon tumor tissues. The 9 amino acid HA sequence was added in frame at the 3′ terminus of GW112 to facilitate Western blot analysis. It was then subcloned into the pAdtrack-CMV vector at the *Eco*R I/*Sal*I sites to produce the pAdtrack-CMV/hGW112 plasmid. Packaging and production of the adenovirus to carry the human *GW112* gene was achieved by use of the AdEasy system according to published protocols (30). This system allows the quick production of E1-deleted recombinant adenovirus vector. Briefly, the pAdtrack-CMV/hGW112 plasmid was linearized by *Pme*I and then recombined with pAdeasy-1 plasmid in recA+ bacteria BJ5183. The resultant pAdeasy containing the human *GW112* gene was then transfected into low passage (<35) 293 cells after have been linearized by *Pac*I to obtain the recombinant adenovirus vector, AdGW112. Successful adenovirus particles usually appear at days 7–12. Large-scale preparation of the virus particles was carried out following established protocols.

Terminal Deoxynucleotidyl Transferase-Mediated Nick End Labeling Assay for *in Situ* Cell Death Detection. The *in situ* cell death detection kit was purchased from Roche Molecular Biology (Mannheim, Germany) and performed according to the user manual. Briefly, SVEC cells are incubated in tissue culture chambers and fixed with a freshly prepared 4% paraformaldehyde solution for 1 h at room temperature after treatments. The slides were rinsed with PBS, and endogenous peroxidase was blocked by use of 3% H_2O_2 in methanol for 10 min. After washing with PBS, the slides are permeabilized with 0.1% Triton X-100 in 0.1% sodium citrate for 2 min on ice, then incubated with terminal deoxynucleotidyl transferase-mediated nick end labeling reaction mixture for 60 min at 37°C. After washing, converter-POD was added onto the slides and the slides were incubated for 30 min at 37°C in a humidified chamber. Around 50–100 μl 3,3′-diaminobenzidine-substrate solution was dropped to the top of the slides and analyzed under a light microscope after incubating for 10 min.

Hochest33342 Stain. HeLa cells were cultured in 12-well plates to 50–60% confluence, and transfected with plasmids by LipofectAMINE (Invitrogen Inc.). The HeLa cells were exposed to 3000 units/ml human IFN-β (Antigenix Corporation, Huntington Station, NY) in combination with 5 μM retinoic acid (RA; Sigma) for 6 days. They were then fixed (methanol:acetic acid; 3:1) for 5 min at 4°C and washed with sterilized dH_2O three times. Subsequently, they were stained with 5 μg/ml Hoechst33342 (Molecular Probes, Eugene, OR) for 10 min at room temperature. Staining was followed by washing three times with sterilized dH_2O. Finally, the slides were mounted with mounting solution (Ref. 24; 0.588% citric acid, 0.71% Na_2HPO4, and 50% glycerol). The stained apoptotic and nonapoptotic nuclei in four randomly selected fields were counted under UV light by two independent investigators.

Western Blot Analysis. The anticaspase-3 and anticaspase-9 antibodies were purchased from Cell Signaling (Beverly, MA). The anti-Bcl-XL and anti-Bcl-2 antibody were purchased from BD PharMingen. After the treatments, cells were collected and lysed. About 250 ng to 2 μg of total protein was electrophoresed on a 7.5–15% SDS-PAGE gel, and then transferred to a nitrocellulose membrane. After blocking the membrane with 5% nonfat milk in(PBS +0.1% Tween 20 overnight at 4°C, the blot was incubated with primary antibody for 1 h, washed with PBS +0.1% Tween 20 three times (15 min each time), incubated with secondary antibody (IgG) conjugated with horseradish peroxidase for 1 h, and washed with PBS +0.1% Tween 20 three times. The signal was visualized with the ECL kit (Amersham, Arlington Heights, IL).

Determination of Cytochrome *C* Release Into Cytosol. To detect the release of cytochrome *c* from the mitochondria to the cytosol, cells are harvested and resuspended in ice-cold lysis buffer (31) and incubated for 10 min on ice. The cell membrane was disrupted by sonicating (5 strokes at 10% duty cycle, 1 output control) by use of a commercially obtained Sonicator (Sonifer 450; VWR Scientific). The lysate was then centrifuged at 750 g for 15 min at 4°C. The supernatant was collected and concentrated by using the microconcentrator (Amicon, Beverly, MA). The pellet containing the mitochondria was dissolved in lyses buffer again and sonicated again. The supernatants were then loaded onto 13.5% SDS-PAGE gels for Western blot analysis with monoclonal anticytochrome *c* antibody (2 μg/ml; BD PharMingen Tech).

Microarray Analysis. The apoptosis array from the Clontech Corporation was used to identify genes induced by IFN-β/RA exposure and modulation of apoptotic gene expression by overexpression of GW112 and GRIM-19. Manufacturer's protocols were followed to carry out the hybridization and analysis.

Reverse Transcription-PCR Analysis. Total RNA was isolated by TRIzol reagent (Invitrogen) and purified by acid-phenol. The reverse transcription was performed by incubating 2–3 μg total RNA, 2.5 μM random primer, and 200 units Superscript II reverse transcriptase (Invitrogen) in 20 μl reaction volume for 1 h at 42°C. PCR amplification was carried out by use of two pairs of primers in the same reaction: one amplifies the particular gene fragment and another amplifies a 1 kb GAPDH fragment that serves as an internal control. To get semiquantitative results, the PCR cycle number was adjusted to anywhere from 25 to 29 (from the usual 32–26). The PCR products were visualized on 1.2% agarose gel containing 0.5 μg/ml ethidium bromide.

Intracellular Localization of Human GW112 and GRIM-19. To determine the intracellular localization of the GW112 protein, pCMV-GW112-HA and pCMV-GRIM19-FLAG plasmid was transfected into HeLa cells cultured in tissue culture chambers by using the LipofectAMINE (Invitrogen). The cells

DOI:10.1158/0008-5472.CAN-03-3443

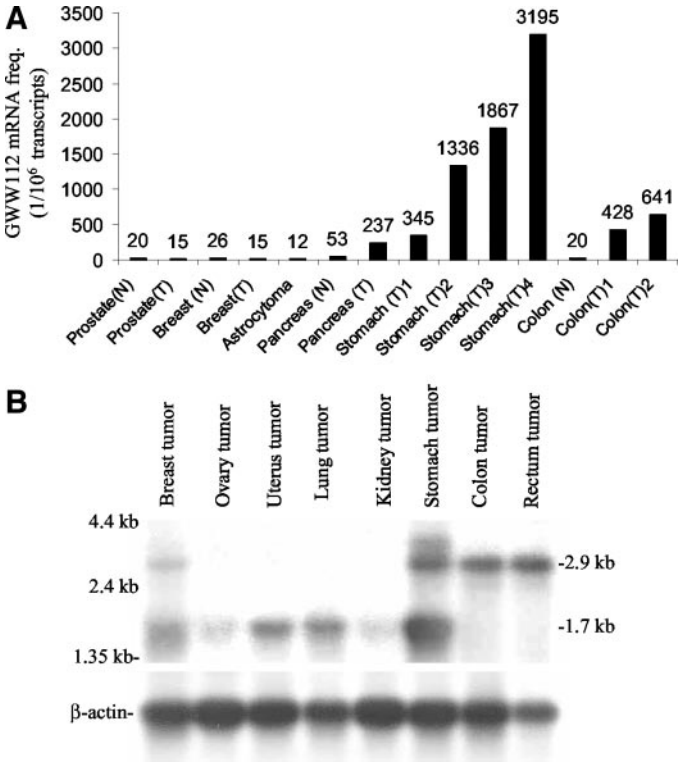

Fig. 1. Distribution of GW112 expression. *A*, a survey of GW112 expression in various normal and tumor tissues. The data were obtained by use of serial analysis of gene expression database available at the National Center for Biotechnology Information. *N*, normal tissue; *T*, tumor tissue. *B*, commercially acquired premade multiple tissues Northern blots (MTN, from Clontech Corporation) were probed with ^{32}P-labeled GW112 and β-actin probes. There was ~10 μg of total RNA per lane, derived from eight human tumor cell lines. The *top panel* shows results from GW112 probe, whereas the *bottom panel* shows results from β-actin cDNA probe

were fixed by 3% paraformaldehyde/2% sucrose, and then permeabilized with ice-cold 1% Triton-X-100 buffer. After blocking with 1% BSA for 30 min at room temperature, the cells were incubated with anti-HA-rhodamine and anti-FLAG-FITC antibodies (5 μg/ml) for 30 min at 37°C, washed with PBS buffer, and viewed under a Zeiss confocal fluorescence microscope.

Clonogenic Assay. HeLa cells at 50–60% confluency were transfected with pCMV-Tag-2B blank plasmid as a control, pCMV-GRIM-19, or pCMV-GRIM-19/pCMV-GW112 (1:1). Fifteen h after transfection, the cells were cultured with 3000 units/ml IFN-β and 5 μM RA for 6 days. About 200 trypsined cells were subsequently plated in 10-cm Petri dishes. About 10–14 days later, colonies that appeared were fixed using methanol and stained with 2% Giemsa solution. All of the colonies with >50 cells were counted. Five replicate dishes were plated for each group. The survival fraction was normalized against those of the control cells. Surviving fraction (SF) was calculated for each treatment as follows:

$$SF = Number\ of\ colonies/$$

$$(total\ number\ of\ cells\ plated) * plating\ efficiency.$$

Plating efficiency of HeLa cells was determined by plating control non-treated cells at 100–200 cells per plate and counting emerging colonies 14 days later.

Tumor Growth Rate Studies. Animal care and experimental procedures were carried out in accordance with institutional guidelines. About 10^7 cells in 50 μl PBS of Tramp-c cells infected with AdGW112 (at a multiplicity of infection of 5) or AdGFP viruses for 15 h were transplanted in the right hind limbs of syngeneic C57BL/6 mice. Over 90% of the cells were infected as evaluated by green fluorescent protein (GFP; which is constitutively expressed from the same AdGW112 vector). Each treatment group consisted of 8–10 animals. Growth curves are plotted as the mean relative tumor volume ± SE *versus* time after implantation. The error bars represent SE.

Statistical Analysis. The quantitative analysis of apoptosis data in Fig. 4*A* and Fig. 5 was carried out by use of Student's *t* test. The data analysis for tumor growth (Fig. 7) was carried out by use of the nonparametric Mann-Whitney test.

RESULTS

The *GW112* gene was identified by virtue of its high expression in colon cancer cells through analysis of Cancer Genome Anatomy Project data from the United States National Cancer Institute. An extensive database search reveals little homology between GW112 and other proteins. There is only a single published report suggesting that it is overexpressed in the crypt epithelium of inflamed colonic mucosa in ulcerative colitis (24). Because of its overexpression in colon cancer cells, we decided to characterize its function by use of a variety of molecular and cell biology approaches.

Expression of GW112 in Normal and Malignant Tissues. To get an idea of the expression profile of GW112 in various tissues, a survey was conducted by use of the serial analysis of gene expression database at the website of National Center for Biotechnology Information. Fig. 1*A* is a summary of the results. It can be seen that GW112 is expressed in several normal tissues (prostate, breast, colon, and pancreas) but at relatively low levels. However, its expression is quite high in pancreatic cancer, stomach cancer, and colon cancer tissues. To additionally confirm the expression of GW112 in various tumors, we carried out Northern blot analysis by use of a ^{32}P-labeled cDNA probe and commercially available MTN blots with RNA from various human tumor tissues. Fig. 1*B* shows the results. Among various tumor tissues, expression of the 2.9 kb species (the predominant species) was seen in those of digestive system origin, rectum, colon, and stomach. It was also seen in breast cancer. Interestingly, a new mRNA species of 1.7 kb, perhaps the result of alternative splicing, was observed in multiple tumors that included breast, ovary, uterus, lung, kidney, and stomach cancers. The exact significance of this new mRNA species is not clear. Only the 2.9 kb species is reported in the GenBank.

Identification of the Proteins That Interact with GW112. To decipher the potential function of GW112, we adopted the yeast two-hybrid system to identify the proteins that interact with GW112. The MatchMaker 3 system with a kidney library from Clontech was used. The kidney library was chosen because no library from the digestive system was available, and normal kidney tissues express low

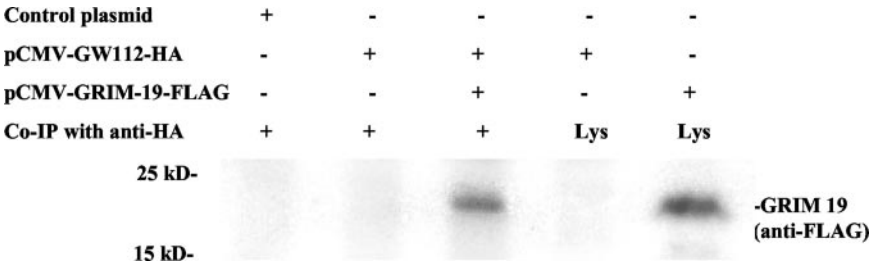

Fig. 2. *In vivo* coimmunoprecipitation of GW112 and GRIM-19 genes. *Lane 1*, pCMV-Tag-2B blank plasmid transfection, immunoprecipitation (IP) with antihemagglutin (HA) antibody; *Lane 2*, pCMV-GW112-HA alone, IP with anti-HA antibody; *Lane 3*, cotransfection of pCMV-GRIM-19-flag and pCMV-GW112-HA, IP with anti-HA antibody, *Lane 4*, pCMV-GW112-HA transfected cell lysate; *Lane 5*, pCMV-GRIM-19 transfected cell lysate.

DOI:10.1158/0008-5472.CAN-03-3443

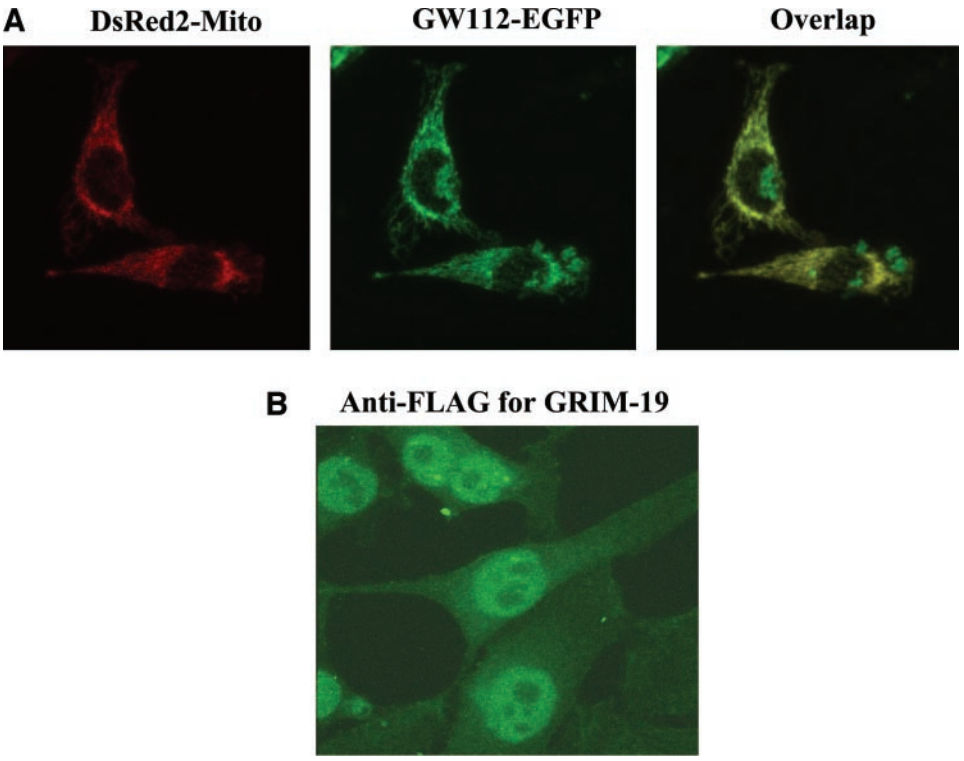

Fig. 3. Intracellular localization of GW112 and GRIM-19. *A*, localization of GW112 to the mitochondria and the nucleus. A plasmid encoding a mitochondria-targeted dsRed2 gene (*pDsRed2-mito*) and a plasmid encoding a GFP-GW112 fusion protein (*pGW112-EGFP*) were cotransfected into HeLa cells. GW112 (*green*) clearly colocalizes with pDsRed2-mito (*red*). In addition, there was clear distribution of GW112 in the nucleus. *B*, localization of the GRIM-19 protein to the nucleus and mitochondria, and so forth. *A*, FLAG-tagged GRIM-19 gene was transduced into HeLa cells, and the location of the GRIM-19 protein was tracked by immunohistochemical staining with an FITC-labeled antibody against the FLAG tag.

levels of the *GW112* gene (data not shown). After stringent screening, 20 independent clones were found to interact with GW112 in the yeast two-hybrid assay. After sequencing these genes, we found that only 10 of the cDNAs were fused to the GAL4 AD correctly, indicating that the other clones were artifacts.

In vivo coimmunoprecipitations between GW112 and these 10 genes were subsequently carried out in mammalian cells by use of engineered genes with short protein tags because of the lack of antibodies. The *GW112* gene was fused with a HA tag derived from the *Influenza* HA protein. The candidate genes were fused with a FLAG tag. Plasmids (with a strong, constitutively active CMV) encoding the two tagged genes were then transfected into 293 cells. Forty-eight h after transfection, the cells were lysed and immunoprecipitation/Western blot analysis was conducted. Only 4 of the 10 genes showed positive coimmunoprecipitation with GW112.

An additional test was conducted for these four proteins by use of the mammalian two-hybrid assay. The one that showed the strongest and most consistent interaction was GRIM-19, a novel apoptosis-related gene involved in retinoic acid-IFN-induced cell death (25–29, 32). Fig. 2 shows the coimmunoprecipitation of GW112 and GRIM-19.

The Intracellular Location of GW112. GRIM-19 has been reported to be a nuclear as well as a mitochondrial protein (25, 28, 29, 32). To determine the location of GW112, we used a reporter gene approach where the *GW112* gene is fused with the GFP gene at the 3′ end. The GW112-GFP fusion gene was then transfected into HeLa cells together with the reporter gene pdsRed2-Mito, which specifically locates to the mitochondria. Fig. 3*A* indicates that almost all of the cytoplasmic GW112-GFP colocalizes with dsRed2-Mito, thereby confirming that cytoplasmic GW112 proteins are mostly localized in the mitochondria. Fig. 3*A* also indicates that GW112 proteins exist in the

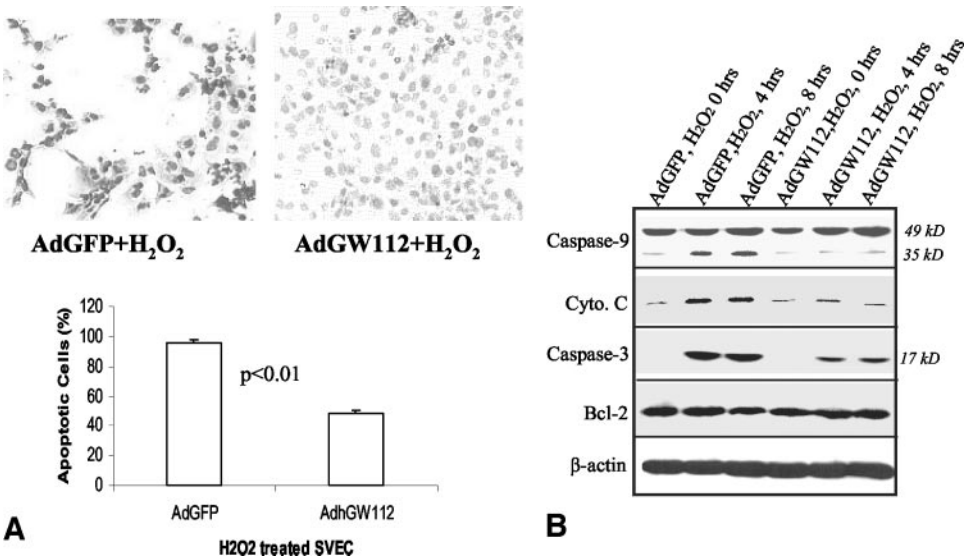

Fig. 4. Attenuation of H_2O_2-induced apoptosis by GW112. *A*, terminal deoxynucleotidyl transferase-mediated nick end labeling evaluation of apoptosis. *Top panels*, photomicrographs of terminal deoxynucleotidyl transferase-mediated nick end labeling-stained, AdGFP- and AdGW112-infected cells that had been treated with 0.8 mM H_2O_2. Those cells with strong, dark nuclear stain were apoptotic. *Bottom panel*, quantitative analysis of apoptosis; *bars*, ±SD. Student's *t* test was used to determine *P*. See text for details. *B*, Western blot analysis of apoptotic proteins in H_2O_2 treated SVEC cells. For caspase-9, the 49-kDa band is the intact form and the 35-kDa band is the cleaved form. For caspas-3, the 17-kDa band is the cleaved form. Notice the difference (for the cleaved forms) between the AdGFP-infected cells *versus* AdGW112-infected cells in SVEC cells. No difference was detected on the Bcl-2 expression.

DOI:10.1158/0008-5472.CAN-03-3443

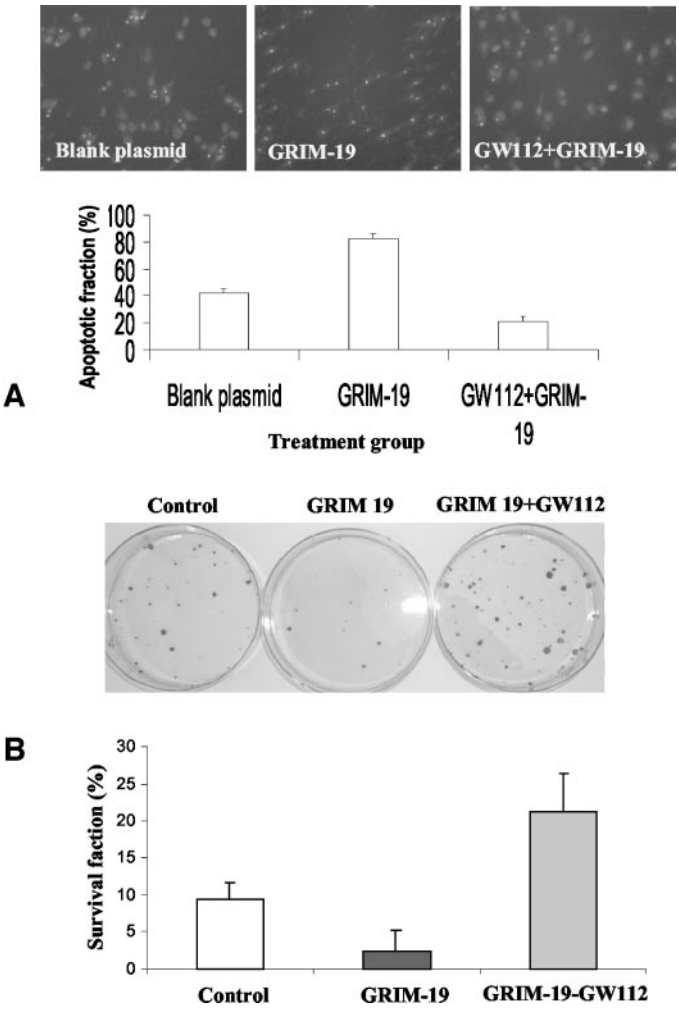

Fig. 5. Attenuation of IFN-β/RA-induced cell death by GW112. *A*, GW112-mediated attenuation of apoptosis in HeLa cells. *Top panel* shows typical photomicrographs of cells under different conditions. The *bottom panel* shows results of quantitative analysis of the extent of apoptosis in different cell populations; *bars*, ±SD among data obtained from three independent Petri dishes with the same treatment. Student's *t* test was used to determine the *P*. *B*, GW112 mediated increase in long-term cellular survival after IFN-β/RA treatment. HeLa cells were transfected with pCMV-Tag-2B blank plasmid as a control; pCMV-GRIM-19, pCMV-GRIM-19, and pCMV-GW112.

nucleus as distinctive foci. To determine the location of the GRIM-19 protein, immunohistochemistry detection was carried out in cells that had been transfected with FLAG-tagged GRIM-19 gene. The result is shown in Fig. 3*B*. It indicates that GRIM-19 is mostly a nuclear protein with cytoplasmic distribution, consistent with earlier reports that GRIM-19 is located both in the nucleus and in the mitochondria (25, 26, 29, 32). Therefore, the interaction of GRIM-19 and GW112 may occur both in the nucleus and in the mitochondria.

Antiapoptotic Properties of GW112. As GRIM-19 is a recognized regulator of apoptosis, we conducted two series of experiments to test whether GW112 is involved in cellular apoptotic pathway. In the first series of experiments, the influence of GW112 on apoptosis was tested in H_2O_2-treated SVEC cells. To evaluate the function of GW112 in H_2O_2-induced apoptosis, an adenovirus AdGW112 encoding the human GW112 cDNA under the control of the CMV promoter was engineered to transduce the *GW112* gene into SVEC cells. The adenovirus-based approach was adopted because it was much more efficient in gene transduction than plasmid-based approaches. When this virus was used to infect SVEC cells, it mediated efficient expression of the *GW112* gene, as determined by a Western blot analysis by use of an antibody to the HA tag fused to the *GW112* gene (data not shown). To evaluate the effects of the GW112 expression on H_2O_2-induced cell death, SVEC cells at 50–60% confluency were infected with AdGFP (control) and AdGW112 at a multiplicity of infection of 10 (which can infect >95% of cells). After 15 h of infection, the cells were treated with 0.8 mM H_2O_2 for 5 h and followed by culturing in normal medium for another 24 h. The cells were then evaluated for viability by use of the terminal deoxynucleotidyl transferase-mediated nick end labeling assay (Fig. 4*A*), which measures the amount of DNA nicks created by apoptotic enzymes. For each treatment, three Petri dishes were evaluated independently. For each dish, 2000 cells from the area with the highest rate of apoptosis were counted. The average from the three dishes was used to represent apoptotic fraction in each treatment group. About 95.8 ± 1.8% of H_2O_2 treated, AdGFP-infected cells appeared apoptotic (similar to uninfected cells). In comparison, 48.3 ± 2.3% of the AdGW112-infected cells showed signs of apoptosis, a significant attenuation in comparison to AdGFP infected cells.

We also examined the downstream pathways that might be affected by GW112 overexpression. SVEC cells at 50–60% confluency were infected with AdGFP (control vector) or AdGW112 at the multiplicity of infection of 10. Fifteen h later, >95% of the cells were infected when examined for GFP expression. The cells were then treated with 0.8 mM H_2O_2 for different lengths of time (4 and 8 h). A series of Western blot analyses were conducted to determine the status of various well-known players in the apoptotic machinery. Fig. 4*B* showed the results. H_2O_2-induced cytochrome *c* release, a hallmark of mitochondria-mediated apoptosis (33–35), was effectively inhibited

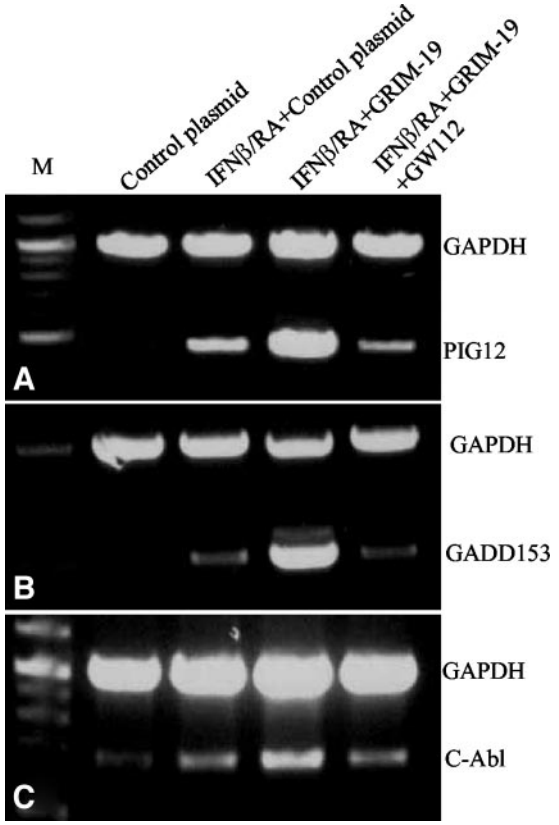

Fig. 6. Semiquantitative analysis of the effects of GW112 and GRIM-19 on IFN-β/RA-induced apoptotic gene expression in HeLa cells. Messenger mRNA from various cell populations were reverse-transcribed into cDNA. The cDNA were then amplified by gene-specific PCR. *A*, the lower band is a PCR-amplified 480 bp PIG12 gene fragment. *B*, the lower band shows a PCR-amplified 512 bp GADD153 gene fragment. *C*, the *lower band* shows a PCR-amplified 671 bp c-Abl gene fragment. The *top bands* in all three panels show the coamplified 1 kb fragment of *GAPDH* gene.

DOI:10.1158/0008-5472.CAN-03-3443

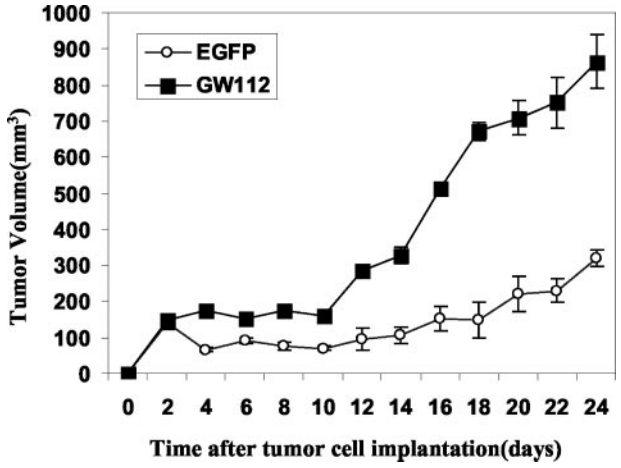

Fig. 7. Tumor growth rate after GW112 gene transduction. After transplantation of 10^7 AdGFP or AdGW112 infected Tramp-C1 cells, tumor size was measured for 24 days (in ○ and ■). GW112 significantly increased the rate of tumor growth ($P < 0.01$); *bars*, ±SE. Nonparametric Mann-Whitney test was use to determine the *P*.

by GW112 expression, as was the activation of caspase 3 and caspase 9, which are the "executioners" of apoptosis. On the other hand, Bcl-2, a potent antiapoptotic protein, showed no change after H_2O_2 treatment in AdGFP as well as AdGW112-infected cells.

In the second series of experiments, we examined the influence of GW112 on apoptosis induced by IFN-β/RA combination. This was because previous reports had indicated that GRIM-19 was a facilitator in apoptosis induced by combined treatment of IFN-β and retinoic acid (25–29). Our efforts to create a GRIM-19 adenovirus failed because of the potential toxicity of GRIM-19 to host cells. Therefore, we adopted a plasmid transfection approach to transduce HeLa cells, which had shown sensitivity to combined IFN-β/RA treatment (25). HeLa cells at 50–60% confluency were transfected with pCMV-Tag-2B blank plasmid, pCMV-GRIM-19, or pCMV-GW112 +pCMV-GRIM-19 (1:1). Fifteen h later, the cells were treated with 3000 units/ml IFN-β and 5 μM RA for 6 days. To evaluate the cell death, cells were then fixed and stained with Hoechest33342. Hoechst33342 dye stains the nucleus of mammalian cells. Apoptotic cells are typically identified as those cells that possess significantly smaller, condensed, and fragmented nuclei under a fluorescence microscope (Fig. 5*A*). About 42.4 ± 2.6% cells exhibited signs of apoptosis in the groups transfected with control plasmids. In comparison, ~82.5 ± 3.6% of the cells appeared apoptotic in the GRIM-19 transfected cells, indicating that overexpression of GRIM-19 efficiently promoted RA/IFN-β induced apoptosis. Interestingly, only 20.8 ± 4.4% of the cells showed signs of apoptosis in the group cotransfected with pCMV-GW112 and pCMV-GRIM-19. These results suggest significant attenuation of GRIM-19-mediated, RA/IFN-β-induced cellular apoptosis by GW112.

To evaluate the influence of GW112 on long-term cellular survival, a clonogenic assay was used to evaluate cellular survival when HeLa cells were exposed to IFN-β/RA. As shown in Fig. 5*B*, pCMV-GRIM-19-transfected cells showed a significantly lower survival (2.6 ± 2.5%; $P < 0.01$) rate when compared with the blank plasmid transfected cells. On other hand, in HeLa cell transfected with pCMV-GRIM-19 and pCMV-GW112, cellular survival increased to 21.5 ± 5.4% ($P < 0.05$). These results are consistent with attenuation of apoptosis observed with Hoechst 33342 staining.

Attenuation of GRIM-19-Mediated Apoptotic Gene Expression by GW112. The above results indicated to us that GW112 could clearly attenuate or block the ability of GRIM-19 to stimulate apoptosis. To additionally elucidate the molecular mechanisms of GW112 and GRIM-19 in apoptosis regulation, we screened for genes up-regulated by GRIM-19 by use of the microarray approach. Three apoptosis-related genes were identified by this approach. These genes are *PIG12* (36, 37), *GADD153* (38–41), and *c-Abl* (42–48). All three of the genes have been reported to be involved in apoptosis and oxidative stress. To additionally verify the expression of these three apoptosis-related genes, total RNA from cells transfected with *GW112* and/or *GRIM-19* genes were extracted and reverse-transcribed. After reverse transcription, PCR amplifications were carried out by use of two pairs of primer in the same reaction: one amplifies the target gene and the other amplifies a 1-kb fragment of the control *GAPDH* gene. Fig. 6 shows the results of semiquantitative reverse transcription-PCR. The expression of all three of the genes was elevated by cellular exposure to retinoic acid/IFN β, indicating potential involvement of the three genes in RA/IFN-β-exposed cells. The elevation of gene expression was additionally enhanced by forced expression of the GRIM-19, which is consistent with its published role in promoting RA/IFN-β-induced cell death. Most importantly, expression of GW112 abolished the up-regulation of gene expression induced by GRIM-19 expression, suggesting its involvement in the same apoptotic pathway as the latter.

GW112 Mediated Enhancement of Clonogenic Survival and Tumor Growth. What is the role of GW112 overexpression in certain tumors? We hypothesized that GW112 is overexpressed in cancer cells to facilitate clonogenic survival and tumor growth. To evaluate the influence of GW112 on cellular survival *in vivo*, the TRAMP-C1 prostate cancer cells, which normally grew slowly after s.c. inoculation (49), were used to assay for their rate of tumor formation. AdGW112 and control AdGFP virus vectors were used to infect TRAMP-C1 cells (at multiplicity of infection of 5 and >90% infection rate). Twenty-four h later, the infected Tramp-C1 cells were injected s.c. into syngeneic C57/BL6 mice. As shown in Fig. 7, tumor volume increased much faster in mice injected with cells infected with AdGW112 ($P < 0.01$). Because AdGFP infection has no effect on tumor growth (data not shown), these results indicate that GW112 overexpression can indeed promote tumor growth *in vivo*.

DISCUSSION

GW112 is a gene initially cloned from human myeloblasts. There is little known about its expression profiles and function. The only report on *GW112* is its preferential expression in the crypt epithelium in inflamed colonic mucosa in ulcerative colitis (24). Our results showed that *GW112* is overexpressed in human tumors, especially in those of the digestive system. It is also interesting to note that different patterns of RNA expression were seen in the experiments. Whereas a single 2.9 kb RNA species was seen in some tumor tissues, an alternatively spliced 1.7-kb RNA transcript as seen in other tumor tissues (Fig. 1*B*). The exact implication of the alternatively splice RNA is unclear.

Because nothing is learned from BLAST comparisons of GW112 with other sequences in GenBank, a yeast two-hybrid system was used to identify the cellular binding partners for it. The identification of GRIM-19 (Figs. 2 and 3) provides revealing information on the potential function of GW112. This is because GRIM-19 is a gene initially identified to be involved in cellular apoptosis induced by IFN-β/RA (25, 28). These studies indicated that GRIM-19 was significantly overexpressed in cells undergoing IFN-β/RA-induced apoptosis. More importantly, the expression of GRIM-19 in HeLa cells directly participated in the apoptotic process. Forced overexpression of the *GRIM-19* gene significantly stimulated IFN-β/RA-induced cell death (Fig. 5). Therefore, the association of GW112 with the GRIM-19 protein suggests that GW112 may be involved in regulating

DOI:10.1158/0008-5472.CAN-03-3443

apoptosis through association with GRIM-19, similar to other proteins that associate with GRIM-19 (28, 29).

A series of experiments indicated that GW112 is indeed involved regulating apoptosis. GW112 was found to attenuate much of the H_2O_2-induced apoptosis. This attenuation was accompanied by inhibition of cytochrome *c* release and caspase activation (Fig. 4), typical signs of mitochondria-initiated apoptosis (33–35, 50). This is consistent with the physical location of the protein, which is largely a mitochondria protein with discreet nuclear distribution (Fig. 3*A*). It is worth noting that its associated protein GRIM-19 is largely a nuclear protein with mitochondrial localization (Fig. 3*B*). Therefore, GRIM-19 and GW112 have distinct but overlapping localization within the nucleus and mitochondria (Fig. 3).

In addition to the suppression of oxidative stress (*i.e.*, H_2O_2)-induced apoptosis, GW112 can also attenuate the effects of GRIM-19 expression in enhancing cellular apoptosis induced by IFN-β/RA-induced apoptosis (25, 27). However, nothing is known about the upstream activators and downstream effectors of GRIM-19 in the IFN-β/RA induced apoptotic pathway. In this study, microarray analysis identified three apoptosis-related genes *Gadd153*, *PIG12*, and *c-Abl* that were up-regulated during IFN-β/RA-induced apoptosis (Fig. 6). The exact significance and mechanism of the up-regulation of these genes are unknown. However, it is interesting that all three of the genes have been implicated in cellular apoptosis induced by genotoxic agents and oxidative stress (36, 38–48). At present nothing is known about the mechanism of GRIM-19 that up-regulates the expression of these genes and how GW112 attenuates their expression. It is possible that the expression of these genes is more downstream of GRIM-19 and their up-regulation is involved in common signal transduction pathways that are involved in apoptosis induced by diverse stress signals. However, the fact that GRIM-19 can enhance the expression of these genes, although GW112 can attenuate the expression of them, provided additional proof that GW112 and GRIM-19 are involved in common pathways of apoptosis regulation.

The antiapoptotic function of GW112 also provides a potential explanation for the overexpression of GW112 in tumors, especially those of the digestive origin. It is possible that GW112 enables tumor cells to overcome the adverse growth conditions of the tumor microenvironment, which is often hypoxic, acidic, or nutrient-deprived. Indeed, forced expression of GW112 allows prostate cancer cells that normally grow very slowly (49) to establish in a much quicker fashion (Fig. 7).

What is the normal physiological function of GW112? We still cannot answer this very important question. However, judging from a previous study that demonstrated overexpression of GW112 in the crypt epithelium of inflamed colonic mucosa in ulcerative colitis and our own data on its antiapoptotic function, we postulate that GW112 may be involved in the regulation of cellular apoptosis under inflammatory conditions in the digestive system.

Taken together, we conclude that GW112 is an important regulator of apoptosis, and its regulation roles are played through the GRIM-19 gene. Its antiapoptotic role may have significant roles in the development of cancer, especially those of digestive system.

ACKNOWLEDGMENTS

We thank Mathew Dreher and Fan Yuan for assistance in confocal microscopy.

REFERENCES

1. Wyllie AH, Kerr JF, Currie AR. Cell death: the significance of apoptosis. Int Rev Cytol 1980;68:251–306.
2. Kerr JF, Wyllie AH, Currie AR. Apoptosis: a basic biological phenomenon with wide-ranging implications in tissue kinetics. Br J Cancer 1972;26:239–57.
3. Vaux DL, Korsmeyer SJ. Cell death in development. Cell 1999;96:245–54.
4. Jacks T, Weinberg RA. Taking the study of cancer cell survival to a new dimension. Cell 2002;111:923–5.
5. Abrams JM. Competition and compensation: coupled to death in development and cancer. Cell 2002;110:403–6.
6. Coultas L, Strasser A. The role of the Bcl-2 protein family in cancer. Semin Cancer Biol 2003;13:115–23.
7. Eng C, Kiuru M, Fernandez MJ, Aaltonen LA. A role for mitochondrial enzymes in inherited neoplasia and beyond. Nat Rev Cancer 2003;3:193–202.
8. Folkman J Angiogenesis and apoptosis. Semin Cancer Biol 2003;13:159–67.
9. Yuan J, Yankner BA. Caspase activity sows the seeds of neuronal death. Nat Cell Biol 1999;1:E44–45.
10. Yuan J, Yankner BA. Apoptosis in the nervous system. Nature (Lond) 2000;407:802–9.
11. Nathan C. Points of control in inflammation. Nature 2002;420:846–852.
12. Stassi G, De Maria R. Autoimmune thyroid disease: new models of cell death in autoimmunity. Nat Rev Immunol 2002;2:195–204.
13. Eguchi K. Apoptosis in autoimmune diseases. Intern Med 2001;40:275–84.
14. Cuconati A, Degenhardt K, Sundararajan R, Anschel A, White E. Bak and Bax function to limit adenovirus replication through apoptosis induction. J Virol 2002;76:4547–58.
15. Cuconati A, White E. Viral homologs of BCL-2: role of apoptosis in the regulation of virus infection. Genes Dev. 2002;16:2465–78.
16. Hanahan D, Weinberg RA. The hallmarks of cancer. Cell 2000;100:57–70.
17. Chau BN, Wang JY. Coordinated regulation of life and death by RB. Nat Rev Cancer 2003;3:130–8.
18. Chene P. Inhibiting the p53-MDM2 interaction: an important target for cancer therapy. Nat Rev Cancer 2003;3:102–9.
19. Smyth MJ, Takeda K, Hayakawa Y, Peschon JJ, van den Brink MR, Yagita H. Nature's TRAIL–on a path to cancer immunotherapy. Immunity 2003;18:1–6.
20. Altieri DC. Validating survivin as a cancer therapeutic target. Nat Rev Cancer 2003;3:46–54.
21. Semenza GL. Hypoxia, clonal selection, and the role of HIF-1 in tumor progression. Crit Rev Biochem Mol Biol 2000;35:71–103.
22. Tannock IF, Rotin D. Acid pH in tumors and its potential for therapeutic exploitation. Cancer Res 1989;49:4373–84.
23. Stratford IJ, Adams GE, Bremner JC, et al. Manipulation and exploitation of the tumour environment for therapeutic benefit. Int J Radiat Biol 1994;65:85–94.
24. Shinozaki S, Nakamura T, Iimura M, et al. Upregulation of Reg 1α and GW112 in the epithelium of inflamed colonic mucosa. Gut 2001;48:623–9.
25. Angell JE, Lindner DJ, Shapiro PS, Hofmann ER, Kalvakolanu DV. Identification of GRIM-19, a novel cell death-regulatory gene induced by the interferon-β and retinoic acid combination, using a genetic approach. J Biol Chem 2000;275:33416–26.
26. Fearnley IM, Carroll J, Shannon RJ, Runswick MJ, Walker JE, Hirst J GRIM-19, a cell death regulatory gene product, is a subunit of bovine mitochondrial NADH: ubiquinone oxidoreductase (complex I). J Biol Chem 2001;276:38345–8.
27. Chidambaram NV, Angell JE, Ling W, Hofmann ER, Kalvakolanu DV. Chromosomal localization of human GRIM-19, a novel IFN-β and retinoic acid-activated regulator of cell death. J Interferon Cytokine Res 2000;20:661–5.
28. Seo T, Lee D, Shim YS, et al. Viral interferon regulatory factor 1 of Kaposi's sarcoma-associated herpesvirus interacts with a cell death regulator, GRIM19, and inhibits interferon/retinoic acid-induced cell death. J Virol 2002;76:8797–807.
29. Lufei C, Ma J, Huang G, et al. GRIM-19, a death-regulatory gene product, suppresses Stat3 activity via functional interaction. EMBO J 2003;22:1325–35.
30. He TC, Zhou S, da Costa LT, Yu J, Kinzler KW, Vogelstein B. A simplified system for generating recombinant adenoviruses. Proc Natl Acad Sci USA 1998;95:2509–14.
31. Walter DH, Haendeler J, Galle J, Zeiher AM, Dimmeler S. Cyclosporin A inhibits apoptosis of human endothelial cells by preventing release of cytochrome C from mitochondria. Circulation 1998;98:1153–7.
32. Murray JG, Zhang B, Taylor SW, et al. The subunit composition of the human NADH dehydrogenase obtained by rapid one step immunopurification. J Biol Chem 2003;28:28.
33. Liu X, Kim CN, Yang J, Jemmerson R, Wang X. Induction of apoptotic program in cell-free extracts: requirement for dATP and cytochrome c. Cell 1996;86:147–57.
34. Yang J, Liu X, Bhalla K, et al. Prevention of apoptosis by Bcl-2: release of cytochrome c from mitochondria blocked. Science (Wash DC) 1997;275:1129–32.
35. Luo X, Budihardjo I, Zou H, Slaughter C, Wang X. Bid, a Bcl2 interacting protein, mediates cytochrome c release from mitochondria in response to activation of cell surface death receptors. Cell 1998;94:481–90.
36. Polyak K, Xia Y, Zweier JL, Kinzler KW, Vogelstein B. A model for p53-induced apoptosis. Nature (Lond) 1997;389:300–5.
37. Jakobsson PJ, Thoren S, Morgenstern R, Samuelsson B. Identification of human prostaglandin E synthase: a microsomal, glutathione-dependent, inducible enzyme, constituting a potential novel drug target. Proc Natl Acad Sci USA 1999;96:7220–5.
38. Zhan Q, Lord KA, Alamo I, Jr, et al. The gadd and MyD genes define a novel set of mammalian genes encoding acidic proteins that synergistically suppress cell growth. Mol Cell Biol. 1994;14:2361–71.
39. Matsumoto M, Minami M, Takeda K, Sakao Y, Akira S. Ectopic expression of CHOP (GADD153) induces apoptosis in M1 myeloblastic leukemia cells. FEBS Lett 1996;395:143–7.

DOI:10.1158/0008-5472.CAN-03-3443

40. Maytin EV, Ubeda M, Lin JC, Habener JF. Stress-inducible transcription factor CHOP/gadd153 induces apoptosis in mammalian cells via p38 kinase-dependent and -independent mechanisms. Exp Cell Res 2001;267:193–204.
41. McCullough KD, Martindale JL, Klotz LO, Aw TY, Holbrook NJ. Gadd153 sensitizes cells to endoplasmic reticulum stress by down- regulating Bcl2 and perturbing the cellular redox state. Mol Cell Biol 2001;21:1249–59.
42. Yuan ZM, Huang Y, Ishiko T, Kharbanda S, Weichselbaum R, Kufe D. Regulation of DNA damage-induced apoptosis by the c-Abl tyrosine kinase. Proc Natl Acad Sci USA 1997;94:1437–40.
43. Theis S, Roemer K. c-Abl tyrosine kinase can mediate tumor cell apoptosis independently of the Rb and p53 tumor suppressors. Oncogene 1998;17:557–64.
44. Cong F, Goff SP. c-Abl-induced apoptosis, but not cell cycle arrest, requires mitogen-activated protein kinase kinase 6 activation. Proc Natl Acad Sci USA 1999;96: 13819–24.
45. Gong JG, Costanzo A, Yang HQ, et al. The tyrosine kinase c-Abl regulates p73 in apoptotic response to cisplatin-induced DNA damage. Nature (Lond) 1999;399: 806–9.
46. Yuan ZM, Shioya H, Ishiko T, et al. p73 is regulated by tyrosine kinase c-Abl in the apoptotic response to DNA damage. Nature (Lond) 1999;399:814–7.
47. Sun X, Majumder P, Shioya H, et al. Activation of the cytoplasmic c-Abl tyrosine kinase by reactive oxygen species. J Biol Chem 2000;275:17237–40.
48. Wang JY. Regulation of cell death by the Abl tyrosine kinase. Oncogene 2000;19: 5643–50.
49. Ciavarra RP, Somers KD, Brown RR, et al. Flt3-ligand induces transient tumor regression in an ectopic treatment model of major histocompatibility complex-negative prostate cancer. Cancer Res 2000;60:2081–4.
50. Yin XM, Wang K, Gross A, et al. Bid-deficient mice are resistant to Fas-induced hepatocellular apoptosis. Nature (Lond)1999;400:886–91.